Contributed paper

OPTO-ELECTRONICS REVIEW 8(3), 263–267 (2000)

Imaging properties of $As_{40}S_{40}Se_{20}$ layers

A.V. STRONSKI*[1] and M. VLČEK[2]

[1]Institute of Semiconductor Physics, NAS Ukraine, 41 Prospekt Nauki, 03028 Kiev, Ukraine
[2]University of Pardubice, 53210 Pardubice, Czech Republic

Here we investigate image formation properties of $As_{40}S_{40}Se_{20}$ layers with regard to their application for gratings fabrication. The light-sensitive properties (photo- and thermally- induced structural changes) of layers have been studied using optical techniques, including Raman spectroscopy. The dissolution kinetics of as-evaporated and exposed layers in amine based etching solutions has been studied. Characteristics of holographic gratings obtained on the base of $As_{40}S_{40}Se_{20}$ layers are presented.

Keywords: $As_{40}S_{40}Se_{20}$ layers, optical properties, Raman spectra, selective etching, holographic diffraction gratings.

1. Introduction

It is well known that exposure to light produces structural changes in chalcogenide amorphous films. As a consequence of such photostructural changes a variety of physical and chemical properties are changed: optical properties, hardness, density, chemical solubility, etc. This determines the numerous possible industrial applications of these materials. Registering media on the base of chalcogenide amorphous films have shown good results in microelectronics [1], high-density information recording [2], holography [3], and diffractive optics [4–5]. This research was motivated by the possibility of application of photosensitive properties of $As_{40}S_{40}Se_{20}$ layers for production of elements of diffraction optics (gratings). The final objective was fabrication of gratings, on the base of such layers, having the parameters comparable with commercially produced ones.

2. Experiment

$As_{40}S_{40}Se_{20}$ glass samples were prepared by melting 5N elements in evacuated silica ampoules. The synthesis was performed using rocking furnace at 700–750°C for 8 to 24 h. The ampoules after synthesis were quenched in a cold water. Films of 0.4–5.0 μm thickness were deposited by the vacuum thermal evaporation ($p = 1\times10^{-3}$ Pa) from the resistance heated silica cruisible onto glass substrates (microscopic slides or blanks for gratings) kept at room temperature. Planetary rotation system used for deposition process improved uniformity in a sample thickness. The deposition rate was measured using a quartz microbalance technique and in the present study was within 1 to 6 nm/s. Samples were kept in complete darkness until treated. Next, they were exposed to different light sources (halogen lamp, natural light, Ar laser). Some samples were annealed in Ar atmosphere at 150°C for 4 hours. Structural changes of variously treated samples (virgin, exposed, annealed) were studied by Raman spectroscopy (FTIR spectrometer IFS55 with FRA 106 Raman module, Bruker, Germany). For the analysis, the Raman spectra have been reduced by the Shuker-Gammon method [6] and normalised by the area. Optical transmittance changes in the ultraviolet-visible--near infrared were measured in the spectral region of 0.3–2.5 μm with a double beam spectrophotometer V-570 JASCO and from these data spectral dependencies of the refractive index $n(\lambda)$, the optical dielectric constant $\varepsilon(0)$, and the single oscillator parameters were estimated. Measurements of selective etching in amine based solutions were carried out using the interference techniques described in Ref. 7. The holographic gratings were recorded in the setup similar to that described in Refs. 4 and 5 using Ar laser radiation. After exposure, selective etching was carried out and after that the reflective layer (Al) was deposited. Diffraction efficiency (relative values) was measured using Littrov scheme. Profiles and relief quality of gratings were studied using a scanning electron microscope.

3. Results

Spectral dependencies the refractive index $n(\lambda)$ for as-evaporated, exposed and annealed films were obtained from the results of transmission measurements. Both exposure and annealing cause increase in the refractive index over the entire spectral region. Analysis of $n(\lambda)$ was carried out within the frame of a single-oscillator model. The parameters of single-oscillator model (the single oscillator energy E_o, the dispersion energy E_d), optical dielectric con-

*e-mail: stronski@isp.kiev.ua

stant and their evolution under exposure and annealing were determined.

Exposure and annealing lead to increase in dielectric constant and decrease in E_o value. The correspondence between E_o and optical band gap energy E_{gopt} obtained from Tauc dependence for $As_{40}S_{40}Se_{20}$ layers can be expressed as $E_o \approx 2E_{gopt}$ which is similar to that observed for As-S compositions [8]. We obtained E_{gopt} values 2.16, 2.11, and 2.05 eV for as evaporated, exposed, and annealed films, respectively. Changes in E_d, in accordance with Ref. 9, indicate the changes in short-range order under exposure or annealing. This can be understood if we take into account that structure of evaporated thin films is somewhat different from the glass one. For example, the structure of the evaporated $As_{40}S_{40}Se_{20}$ film can be represented in form of matrix, which consists of the pyramidal units $AsS(Se)_{3/2}$. This matrix contains considerable amounts of $As_4S(Se)_4$ and $S(Se)_2$ fragments that contain As-As and S(Se)-S(Se) "wrong" bonds. Other defects, pores can be present in the structure as well. Raman spectra of fresh evaporated $As_{40}S_{40}Se_{20}$ layers show the presence of several narrow bands that correspond to As rich and S(Se) rich fragments. Annealing and exposure results in polymerisation of the molecular groups in the main glass matrix, thus the number of homopolar bonds defects is diminished. That is clearly seen in Raman spectra (Fig. 1) where under annealing or with increase in exposure dose the bands corresponding to the homopolar bonds (122, 135, 147, 168, 176, 189, 201, 222, and 495 cm^{-1}) are decreased and the spectra are nearing towards the bulk ones (where the two intensive and broad bands near 253 and 348 cm^{-1} are the dominant features). This results in increase in relative density of main structural units $AsS(Se)_{3/2}$, that provides the higher values of E_d, 20.0 and 19.6 for annealed and exposed layers, correspondingly (for unexposed layer E_d = 18.1). Intensity decrease in exposure of the 189 cm^{-1} band, corresponding to the presence of homopolar bonds, can be described by exponential decay function (Fig. 2).

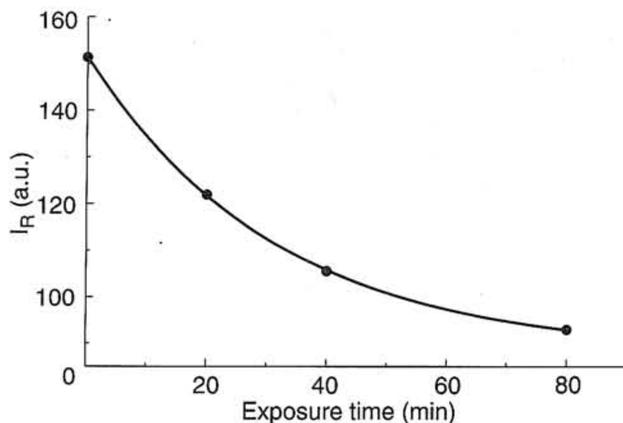

Fig. 2. Dependence of intensity I_R of 189 cm^{-1} Raman band on exposure (data from Fig. 1).

The etching properties of as-evaporated and exposed $As_{40}S_{40}Se_{20}$ thin films in amine based etching solutions (in particular, nonaqueous solutions based on triethylamine, Fig. 3) were investigated using various techniques, including the optical ones. It can be seen in Fig. 3 that $As_{40}S_{40}Se_{20}$ layers have good ability to modify their solubility in amine based solutions by exposure to light (UV, VIS, etc.). After exposure solubility change can be as high as 8–25, depending on exposure value (curves 2 and 3). The selective etching is mostly near surface limited, that is connected with value of the light penetration depth (see change of etch rate in curves 2 and 3). This feature of the selective etching processes is essential for the films with thickness ≥ 1 μm, where after removal of the near surface layer with changed solubility the etch rate nears to the one

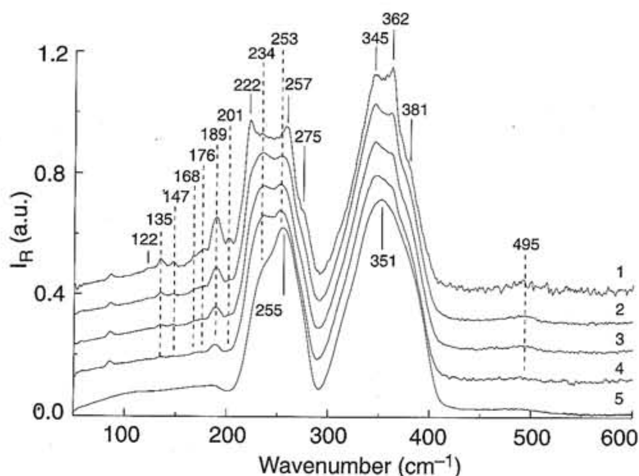

Fig. 1. Raman spectra of $As_{40}S_{40}Se_{20}$, 1- as-evaporated layer, 2, 3, 4-exposed (halogen lamp, I = 20 mW/cm^2, IR cutoff filter) 20, 40, 80 min of exposure, respectively; 5-bulk glass. Raman spectra have been reduced by the Shuker-Gammon method [6], normalised by area and shifted.

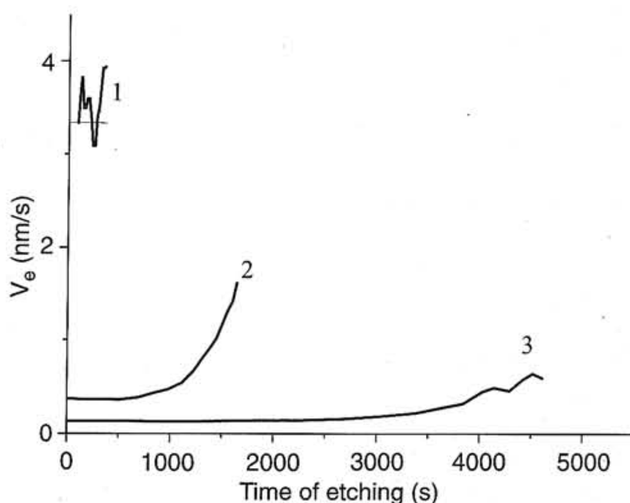

Fig. 3. Dependence of etch rate of $As_{40}S_{40}Se_{20}$ layer (initial thickness ~1200 nm) in non-aqueous etching solution on the base of triethylamine on the time of etching: 1-as- evaporated layer, 2, 3-exposed (halogen lamp, I = 20 mW/cm^2, IR cutoff filter), 2 and 12 min, respectively.

© 2000 COSiW SEP, Warsaw

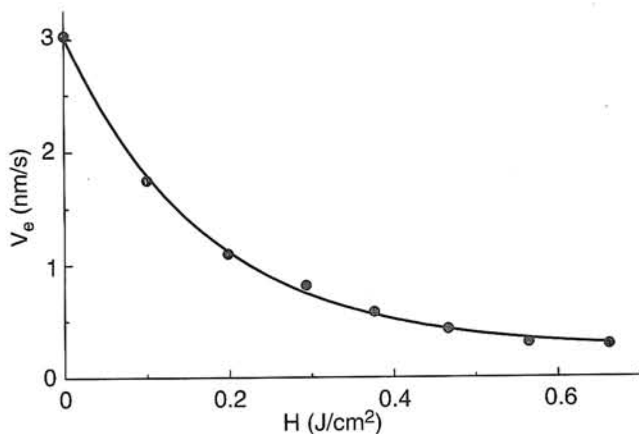

Fig. 4. Dependence of etch rate of $As_{40}S_{40}Se_{20}$ layer in non-aqueous amine-based etching solution on exposure (Ar laser, 488 nm).

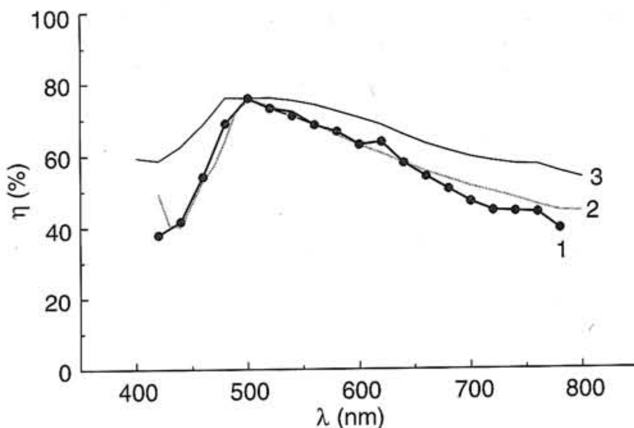

Fig. 6. Spectral distribution of the diffraction efficiency for the gratings with spatial frequency 1800 mm^{-1}: 1– grating on the base of $As_{40}S_{40}Se_{20}$ layer, 2 – data from Ref. 14, 3- data from Ref. 15. Non-polarised light, relative units.

characteristic for unexposed layer [10]. Dependence of etching rate of $As_{40}S_{40}Se_{20}$ films on the exposure H is well described by exponential decay dependence (Fig. 4). The light sensitivity values for them may be as high as 10–14 cm^2/J with contrast values up to 1. The $As_{40}S_{40}Se_{20}$ films provide good etching selectivity and can be successfully used as it was already said above for fabrication of surface-relief patterns.

Conditions of gratings recording were optimised using numerical modelling of the relief formation processes and approach shown in Ref. 4. The optimisation procedure is necessary because the surface-relief of the developed layer is not linearly dependent on the recorded intensity pattern. The profiles resulting from holographic exposure and treatment (mainly cycloidal, sinusoidal, and truncated cycloid) depend on many parameters such as recording laser wavelength, intensity pattern, parameters of $As_{40}S_{40}Se_{20}$ layer, etching characteristics of the developer, thickness of the initial layer, etc. This provided good quality of gratings surface relief (Fig. 5) and modulation depth necessary for obtaining of high values of diffraction efficiency which was measured in the Littrov scheme (relative units). The diffraction efficiency η values for holographic gratings with spatial frequency 1800 mm^{-1} obtained with use of $As_{40}S_{40}Se_{20}$ layers consist ~76% in maximum of η spectral dependence for non-polarised light (Fig. 6).

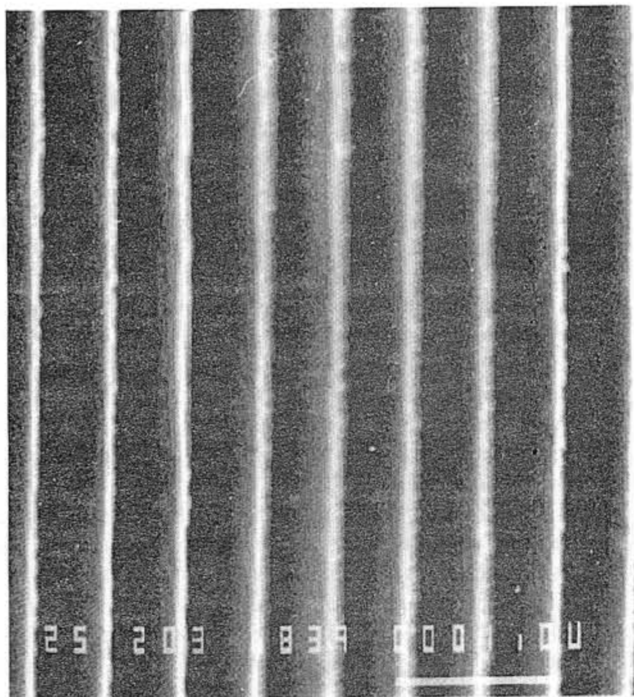

Fig. 5. SEM image of holographic grating with spatial frequency 1800 mm^{-1} fabricated with the use of $As_{40}S_{40}Se_{20}$ layer as recording media.

4. Discussion

Molecular fragments observed in as-evaporated $As_{40}S_{60-X}Se_X$ films are related to the molecular composition of vapour, which is partially frozen during condensation onto substrate. In $As_{40}S_{40}S_{20}$ vapour various $As_mS(Se)_n$, $S(Se)_n$ clusters can be present. During condensation these molecular fragments recombine with each other to form network with bond distribution close to a random one. Thus in as-evaporated films homopolar bonds as well other defective bonds are present (dangling or nonterminating). Concentration of molecular fragments containing homopolar bonds in as-evaporated As_2S_3 and As_2Se_3 layers was estimated as ~30 at% [11,12]. As the photon energy approaches zero the refractive index becomes dependent on the dispersion energy E_d according to the single-oscillator model [9]. The dispersion energy E_d in this case is mainly affected by short-range order, i.e., by nearest-neighbours and the changes in E_d under exposure or annealing correspond to the changes in short-range order. The exposure or annealing of the films leads to the stabilisation of the local structure through redistribution of the chemical bonds of nearest environment. Under exposure the interaction be-

tween As-As and S(Se) rich molecular fragments takes place with the increase of the number of $AsS(Se)_{3/2}$ structural units. There is no significant influence of the diffusion processes, because due to high concentration of As-As and S(Se) rich molecular fragments (as was said above $\geq 30\%$) in initial as-evaporated films they are in nearest environment to each other (in cube with a side length of ~2 atoms). It was also noted that in amorphous chalcogenides photo-excited carriers are rapidly localised to a range of a few angstroms with resulting recombination-induced bond rearrangements [13]. Such bonds rearrangements with decrease of homopolar bonds are favoured thermodynamically. Thus, the change of the number of As-As and S(Se) rich molecular fragments N_H and, respectively, the number of homopolar bonds at light exposure can be written as

$$dN_H / dt = -C\alpha I N_H, \qquad (1)$$

where α is the absorption coefficient, I is the light intensity, and C is the constant.

Solution of Eq. (2) gives

$$N_H = N_{H0} \exp(-C\alpha H), \qquad (2)$$

where N_{H0} is the number of As-As and S(Se) rich molecular fragments (and number of respective homopolar bonds) in the initial as-evaporated film, H = It is the exposure value. Such consideration is supported by the exponential decay dependence shown in Fig. 2. Exponential decay dependence of the etching rate, V_e, on exposure may be considered connected with similar dependence (2) of the number of molecular fragments on exposure but here it is necessary to note that during dissolution of $As_{40}S_{40}Se_{20}$ layers etching of stoichiometric molecular fragments $AsS(Se)_{3/2}$ and non-stoichiometric As-As and S(Se) rich molecular fragments can proceed in several stages, different mechanisms are possible and thus interconnection of V_e and N_{H0} can be more complex.

Amine based etching solutions (in particular based on triethylamine) provide necessary selectivity and good quality of the surface relief which can be seen in Figs. 3 and 5. Etching selectivity is important during transfer of the exposure pattern to a surface-relief profile, because in order to obtain the high values of the diffraction efficiency it is essential to fabricate the necessary depth and form of the relief profile.

Optimisation of the relief formation processes enables the production of the gratings with high values of the diffraction efficiency. It can be seen from Fig. 6 that maximal η value coincide with those presented in catalogues of leading firms [14,15]. Our data (curve 1) on spectral distribution of η practically coincide with those presented in Jobin-Yvon catalogue (curve 3) [15]. Somewhat smaller η values on the wings of operational range in comparison to curves 2 is connected with smaller modulation depth h/d (h is the relief depth, d is the grating period) of grating in our case (~0.3) as compared with 0.36 for curve 2 [14].

5. Conclusions

The investigations that have been carried out demonstrate that the level of photostructural transformation in $As_{40}S_{40}Se_{20}$ layers provide their acceptable sensitivity, adequate etching selectivity and the formation of the high-quality grating surface relief. $As_{40}S_{40}Se_{20}$ layers provide fabrication of holographic gratings with efficiency parameters close to the industrially produced ones and thus can be used as recording media for holography as well.

References

1. A.V. Stronski, "Production of metallic patterns with the help of high resolution inorganic resists," in *Microelectronic Interconnections and Assembly NATO ASI Series* 3, *High Technology* **54**, pp. 263–293, edited by G. Harman and P. Mach, Kluwer Academic Publishers, Netherlands, 1998.
2. I.Z. Indutnyi, S.A. Kostioukevitch, V.I. Minko, P.E. Shepeljavi, and A.V. Stronski, "Application of inorganic resists in high density information storage technologies," *Proc. SPIE* **2451**, 456–467 (1995).
3. I.I. Robur, P.F. Romanenko, A.V. Stronski, L.A. Kostrova, P.E. Shepeljavi, and S.A. Kostioukevitch, "Chalcogenide layer as a holographic media," *Proc. SPIE* **1983**, 593–594 (1993).
4. A.V. Stronski. P.F. Romanenko, I.I. Robur, I.Z. Indutnyi P.E. Shepeljavi, and S.A. Kostioukevitch, "Recording of holographic optical elements on As-S-Se layers," *J. Inf. Rec. Mats.* **20**, 541–546 (1993).
5. I.Z. Indutnyi, A.V. Stronski, S.A. Kostioukevitch, P.E. Schepeljavi, P.F. Romanenko, and I.I. Robur, "Holographic optical element fabrication using chalcogenide layers," *Opt. Eng.* **34**, 1030–1039 (1995).
6. R. Shuker and R.W. Gammon, "Raman-scattering selection-rule breaking and the density of states in amorphous materials," *Phys. Rev. Lett.* **25**, 222–225 (1970).
7. M. Frumar, M. Cvrkal, M. Vlček, and T. Wagner, "The photostructural changes and reactivity of chalcogenide layers," *J. Non-Cryst. Solids* **164–166**, 1243–1246, (1993).
8. K. Tanaka, "Optical properties and photoinduced changes in amorphous As-S films," *Thin Solid Films* **66**, 271–279 (1980).
9. S.H. Wemple, "Refractive index behaviour of amorphous semiconductors and glasses," *Phys. Rev.* B **77**, 3767–3777 (1973).
10. A.V. Stronski, M. Vlček, J. Prokop, T. Wagner, S.A. Kostioukevitch, and P.E. Shepeljavi, "As-S thin films as inorganic resists and some their applications," *Proc. of Ukrainian Vacuum Society* **3**, 235–237 (1997).
11. F. Kosek, Z. Cimpl, J. Tulka, and J. Chlebny, "New analytic method for investigation of the distribution of bonds in As-S systems," *J. Non-Cryst. Solids* **90**, 401–404 (1987).
12. N.D. Aksenov, L.L. Makarov, and S.B. Mamedov, "Chemical ordering in As_2Se_3 films under photostructural transformations," *Non-Crystalline Semiconductors*-**89**, Uzhgorod, Patent, 192–194 (1989).
13. H. Fritzsche, "The origin of reversible and irreversible photostructural changes in chalcogenide glasses," *Phil. Mag.* **68**, 561–572 (1993).

© 2000 COSiW SEP, Warsaw

14. *Diffraction Gratings 1999 Products Guide Richardson Grating Laboratory*, Rochester, New York, 14605 USA; *Diffraction Grating Handbook, Richardson Grating Laboratory*, edited by C. Palmer and E. Loewen, 65PP, 1996, Diffraction grating handbook, second ed., edited by C. Palmer and E. Loewen, Milton Roy Company, USA, 66PP, 1994.

15. *Guide For Spectroscopy ISA JOBIN-YVON 1993*, France-Compo- Photo, 167PP; Nouvelles caracteristics des reseaux de diffraction Jobin-Yvon, 16-18 Rue du Canal, 91160 Longjumeau, France; *Diffraction Gratings Ruled and Holographic-Handbook*, Instruments SA Inc., 173 Essex Avenue, Metuchen, N.J., USA, and ISA-Jobin-Yvon, 16-18 Rue du Canal, 91160 Longjumeau, France.